REGULAR ARTICLE

blood VTH
vessels, thrombosis & hemostasis

Unfolded von Willebrand factor binds protein S and reduces anticoagulant activity

Martha M. S. Sim,[1] Molly Y. Mollica,[2-4] Hammodah R. Alfar,[1] Melissa Hollifield,[5] Dominic W. Chung,[2,6] Xiaoyun Fu,[2,3] Siva Gandhapudi,[5] Daniëlle M. Coenen,[1] Kanakanagavalli Shravani Prakhya,[1] Dlovan F. D Mahmood,[7] Meenakshi Banerjee,[1] Chi Peng,[8] Xian Li,[7] Alice C. Thornton,[9] James Z. Porterfield,[5,9] Jamie L. Sturgill,[5] Gail A. Sievert,[10] Marietta Barton-Baxter,[10] Ze Zheng,[11,12] Kenneth S. Campbell,[10] Jerold G. Woodward,[5] José A. López,[2,3] Sidney W. Whiteheart,[1,7] Beth A. Garvy,[5] and Jeremy P. Wood[1,7,13]

[1]Department of Molecular and Cellular Biochemistry, University of Kentucky, Lexington, KY; [2]Bloodworks Northwest Research Institute, Seattle, WA; [3]Division of Hematology, School of Medicine, University of Washington, Seattle, WA; [4]Department of Mechanical Engineering, University of Maryland Baltimore County, Baltimore, MD; [5]Department of Microbiology, Immunology and Molecular Genetics, University of Kentucky, Lexington, KY; [6]Department of Biochemistry, University of Washington, Seattle, WA; [7]Saha Cardiovascular Research Center, University of Kentucky, Lexington, KY; [8]Department of Pharmacology and Nutritional Sciences, University of Kentucky, Lexington, KY; [9]Division of Infectious Disease, University of Kentucky, Lexington, KY; [10]Center for Clinical and Translational Science, University of Kentucky, Lexington, KY; [11]Department of Medicine, Medical College of Wisconsin, Milwaukee, WI; [12]Versiti Blood Research Institute, Milwaukee, WI; and [13]Division of Cardiovascular Medicine Gill Heart and Vascular Institute, University of Kentucky, Lexington, KY

Key Points

- VWF binds PS in a shear-dependent manner, reducing the free PS pool and its anticoagulant activity.
- The PS/VWF complex forms under turbulent flow conditions, is stable in whole blood, and localizes to growing platelet thrombi.

The critical plasma anticoagulant protein S (PS) circulates in 2 functionally distinct pools: free (anticoagulant) or bound to complement component 4b-binding protein (C4BP; anti-inflammatory). Acquired free PS deficiency is detected in several viral infections, but its cause is unclear. Here, we used biochemical approaches and human patient plasma samples to identify an interaction between PS and von Willebrand factor (VWF), which causes free PS deficiency and reduced PS anticoagulant activity. We first identified a shear-dependent interaction between PS and VWF by mass spectrometry. Consistently, PS and VWF could be crosslinked together in plasma, and plasma PS and VWF comigrated in gel electrophoresis. The PS/VWF interaction was blocked by and tissue factor pathway inhibitor but not activated protein C, suggesting an interaction with the sex hormone binding globulin region of PS. Microfluidic systems demonstrated that PS stably binds VWF as VWF unfolds under turbulent flow. PS/VWF complexes also localized to platelet thrombi under laminar arterial flow. In thrombin generation–based assays, shearing plasma decreased PS activity, an effect not seen in the absence of VWF. Finally, free PS deficiency in patients with COVID-19 correlated with changes in VWF, but not C4BP, and with thrombin generation. Our data indicate that PS binds to a shear-exposed site on VWF, thus sequestering free PS and decreasing its anticoagulant activity, which would account for the increased thrombin generation potential. Because many viral infections present with free PS deficiency, elevated circulating VWF, and increased vascular shear, we propose that the PS/VWF interaction reported here is a likely contributor to virus-associated thrombotic risk.

Introduction

Hemostasis is a tightly regulated balance of procoagulant proteins, which promote the activation of thrombin and the formation of a fibrin clot, and anticoagulant proteins, which terminate this process.[1]

Submitted 10 June 2024; accepted 8 September 2024; prepublished online 25 September 2024. https://doi.org/10.1016/j.bvth.2024.100030.

All data included in this study are available from the corresponding author, Jeremy P. Wood (jeremy.wood@uky.edu), upon request.

The full-text version of this article contains a data supplement.

Thrombosis occurs due to a dysregulation of this balance, caused either by increased procoagulant activity, decreased anticoagulant activity, or both. Protein S (PS) is a critical anticoagulant protein, present in plasma and platelet α-granules,[2] deficiency of which is associated with increased thrombotic risk.[3] Plasma PS exists in 2 pools. Approximately 40% is considered "free PS" and has anticoagulant activity.[4] It is a cofactor for activated protein C (APC), which degrades factors Va and VIIIa,[5] and tissue factor pathway inhibitor α (TFPIα), which inhibits factors VIIa and Xa.[6] PS also directly inhibits factor IXa.[7] The remaining ~60% of plasma PS is bound to the β-chain of complement component C4b-binding protein (C4BP-β).[4] C4BP stabilizes PS, preventing its clearance,[8] and blocks most anticoagulant activity.[9] Acquired PS deficiency is a common complication of severe viral infections, including HIV,[10,11] varicella,[12] dengue,[13] and severe acute respiratory syndrome coronavirus 2 (SARS-CoV-2),[14-19] all of which are associated with an increased risk of thrombosis.

There are 2 broad categories of acquired PS deficiency: reduced total PS or selectively reduced free PS. Although the causes of total PS deficiency are varied (eg, decreased synthesis, increased consumption, or degradation[18]), the causes for loss of free PS are unclear. Because total PS is unchanged, free PS deficiency is thought to indicate the presence or increase of a PS-binding protein. The most widely studied example of this is C4BP, which coprecipitates with PS with polyethylene glycol (PEG).[20] However, although C4BP does increase during inflammation, the change is primarily C4BP α-chain, as opposed to the PS-binding β-chain.[21]

The same infectious disease conditions described above are also associated with concomitant increases in von Willebrand factor (VWF).[22-25] However, whether these 2 hemostatic alterations occur coincidentally or are mechanistically linked is unknown. VWF, in its shear-induced unfolded state, binds several blood proteins, including platelet glycoprotein Ib (GPIb)[26] and ADAMTS13.[27] VWF unfolding is regulated by both shear force and multimer size, with larger multimers unfolding more readily.[28] Either of these factors can be altered during infection.

Here, we focused on identifying PS binding partners in plasma. We demonstrate that PS interacts with VWF in a shear-dependent manner. Sheared VWF blocks the detection of free PS and reduces PS anticoagulant activity in human plasma. Additionally, the PS/VWF complex forms as VWF unfolds under flow, is stable under arterial flow conditions, and localizes to growing platelet thrombi. Finally, we show the potential clinical relevance of our observations in a cohort of patients with SARS-CoV-2, who presented with free PS deficiency that correlated with increased VWF and thrombin generation. Based on our data, we propose a mechanism of free PS deficiency under inflammatory conditions, in which the increased presence of shear-unfolded VWF sequesters PS, thereby limiting its anticoagulant activity.

Methods

Study population and sample isolation

Human participant studies were approved by the Institutional Review Board of the University of Kentucky, and the procedures followed were per the Declaration of Helsinki. Written informed consent was received from patients before participation. Blood samples were collected from adults: SARS-CoV-2–negative controls (n = 38; 56% male and 44% female; age, 59.9 ± 14.1 years) and hospitalized patients with SARS-CoV-2 (COVID-19) (n = 30; 69% male and 31% female; age, 61.5 ± 14.2 years). Participants were enrolled between April 2020 and January 2021 through the Kentucky Clinic and the University of Kentucky Center for Clinical and Translational Science. Some samples were collected after participants had received the SARS-CoV-2 vaccine. Blood was collected, and plasma was isolated as described.[29] For some experiments, samples were also obtained from outpatients with SARS-CoV-2 (patients with mild or no symptoms, after quarantine; n = 5; 40% male and 60% female; age, 48.4 ± 15.5 years).

Statistics

Statistical analyses were performed using GraphPad Prism version 9.5.1. Grouped data were analyzed by nonparametric Mann-Whitney tests (2 groups) or Kruskal-Wallis followed by Dunn multiple comparisons tests (>2 groups), and correlation coefficients were calculated by the method of Spearman, unless otherwise noted in figure legends (Figure 3).

Additional methods and materials can be found in supplemental Data.

Results

VWF interacts with PS in a shear-dependent manner

To identify proteins that interact with VWF in a shear-dependent manner, plasma samples were incubated with VWF-derivatized beads. To induce shear-dependent unfolding, samples were subjected to vortex mixing for 30 minutes, and bound proteins were identified by mass spectrometry. In all 3 plasma samples (2 pooled and 1 single-donor), vortexing increased the quantity of PS bound to VWF (>10 000 000-fold in 2 of 3 samples), suggesting that shear-induced unfolding of VWF exposes a PS-binding site (Figure 1A-B). By comparison, albumin and fibrinogen only increased twofold to fourfold after vortexing. C4BP-α was also enriched (Figure 1C; supplemental Figure 1), though to a lesser extent than PS (5-fold to 38-fold). However, C4BP-β, the PS-binding subunit, was not detected, suggesting that C4BP-bound PS does not bind sheared VWF. Factor VIII was also not detected, likely because it remained tightly bound to plasma VWF and did not transfer to the beads under the conditions used. There was <2-fold increase in VWF-specific peptides, indicating that plasma VWF also did not bind to the VWF-derivatized beads, possibly due to the inhibitory effect of plasma high-density lipoprotein on VWF self-association.[30]

PS/VWF complex forms under turbulent flow conditions

To investigate whether PS directly binds VWF and whether the complex forms under conditions of turbulent flow, we used a polydimethylsiloxane microfluidic device[30] that allows for visualization of VWF self-association around the polydimethylsiloxane block (Figure 2A). VWF and fluorescently labeled PS were perfused into the microfluidic device in the absence (Figure 2B; supplemental Figure 2A; supplemental Videos 1 and 2) or presence (Figure 2C; supplemental Figure 2B; supplemental Videos 1 and 2) of 2 mM calcium chloride. Both PS and VWF have calcium-sensitive features[31-33]; thus, we assessed the effects of calcium on the PS/VWF interaction using purified proteins. We observed

A

Ratio of shear/static binding to VWF-beads

	Pooled Plasma 1	Pooled Plasma 2	Single Donor
VWF	2	2	2
PS	$18.8x10^6$	5	$13.0x10^6$
C4BP-α	38	5	9
ApoA1	13	5	13
Albumin	4	2	3
Fibrinogen*	3	1	2

*Fibrinogen α, β, and γ chains

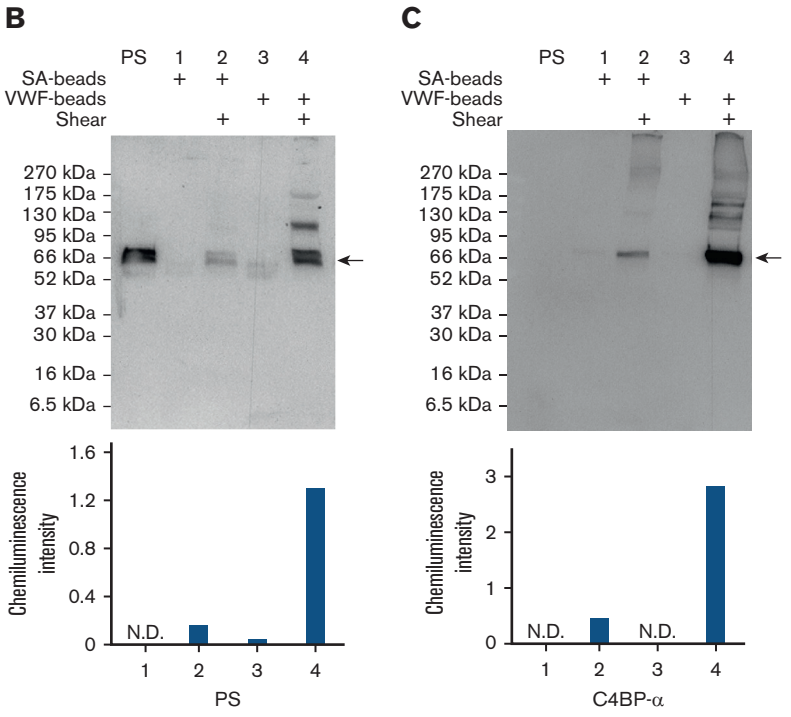

Figure 1. Sheared VWF interacts with PS in plasma and interferes with free PS measurement. Streptavidin beads–immobilized biotinylated VWF was exposed to pooled human plasma or single donor plasma, under static conditions or under shear (vortexing), and bound proteins were analyzed with nanoLC-MS/MS, and probed for PS and C4BP-α by immunoblot, with SA used as a control. (A) Mass spectrometry analysis of VWF pull down in pooled normal plasmas (pooled plasma 1 from Innovative Research; pooled plasma 2 from Precision Biologics) and single donor. (B-C) Western blot of VWF pull down probed for PS (B) and reprobed for C4BP-α (C). Arrows indicate the bands used for densitometric analysis. LC-MS, liquid chromatography-mass spectrometry, SA, serum albumin.

PS binding to VWF under shear and found that PS binding was significantly higher in the absence of calcium (Figure 2C). As expected, we observed no fluorescence intensity over background in the absence of VWF or PS (Figure 2C; supplemental Figure 2C; supplemental Videos 1 and 2). To account for differences in VWF self-association with and without calcium, we normalized PS binding to the area of VWF self-association in each channel. Even with normalization, PS binding was significantly higher in the absence of calcium (Figure 2D).

Microfluidics experiments were also performed under laminar arterial conditions to visualize PS and VWF on thrombi formed under shear. Whole blood was supplemented with fluorescently tagged PS and VWF, either with or without prior shearing, recalcified, and perfused at 35 dyn/cm^2 (approximately arterial) shear stress (Figure 3). In the absence of prior shearing, no apparent colocalization of PS and VWF was observed, because PS and VWF bound independently to different thrombi structures ($r = 0.177$). When whole blood was supplemented with the preformed PS/VWF complex, the 2 proteins colocalized on growing platelet thrombi ($r = 0.355$), indicating that the complex is stable under flow and that PS does not block VWF from binding platelet GPIb. However, arterial laminar flow did not induce complex formation alone.

Unfolded VWF reduces PS anticoagulant activity

The effect of VWF binding on PS anticoagulant activity was measured using plasma thrombin generation in the presence or absence of exogenous APC (5 nM), as described by Brugge et al,[34] with or without vortexing to generate shear (Figure 4A). The data were expressed as percent reduction in peak thrombin upon APC addition. In pooled plasma, APC reduced peak thrombin by 72.0% ± 7.1%. By contrast, a 3.0% ± 3.5% reduction was observed in PS-immunodepleted plasma. Vortexing plasma decreased the apparent anticoagulant activity, because APC only reduced peak thrombin by 56.0% ± 7.8% ($P = .005$). Similar results were observed in plasma from an individual donor. This reduction was entirely dependent on PS, because APC had no effect in vortexed PS-immunodepleted plasma (1.7% ± 1.0% reduction; $P = .497$). The effect was also dependent on VWF. In type 3 von Willebrand disease plasma, PS had increased apparent anticoagulant activity (reducing the peak by 87.2% ± 3.3%), which was not changed by vortexing (83.2% ± 0.5%). Thus, PS activity was not altered by vortexing in the absence of VWF.

Next, we used a recently described PS-sensitive thrombin generation assay that relies on in situ protein C activation (Figure 4B-C).[11] In contrast to the APC experiments, vortexing plasma for 1 minute had little effect on anticoagulant activity. However, vortexing for 1 hour, to maximize VWF unfolding, resulted in decreased APC/PS activity. Similar to the exogenous APC experiments, this reduction was dependent on PS and VWF. Collectively, the in vitro data indicate that unfolded VWF binds PS, reducing the concentration of free PS and decreasing PS anticoagulant activity.

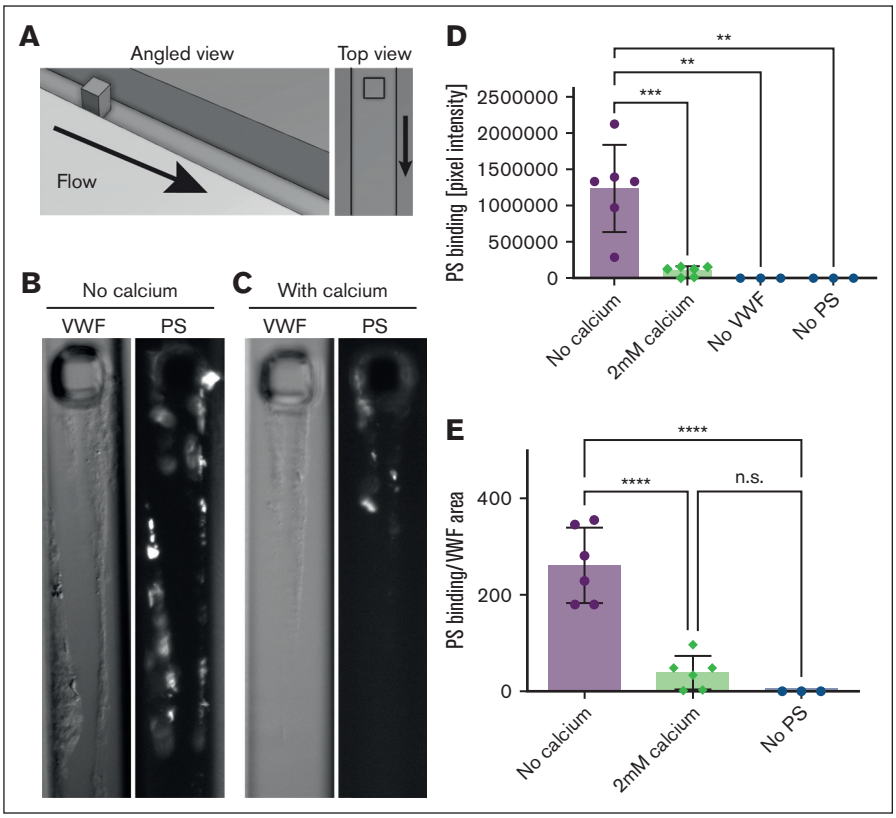

Figure 2. PS binds to VWF that unfolds during disrupted flow conditions in a calcium-modulated manner. (A) VWF and PS were perfused through a PDMS microfluidic device. (B-C) In the absence (B) or presence of 2 mM calcium (C), VWF self-association and Alexa Fluor 488-PS binding were visualized by DIC and epifluorescence microscopy, respectively. (D) Raw pixel intensity above noise was summed for these conditions and controls without VWF (with PS) and without PS (with VWF). Each data point indicates an independent run. (E) When accounting for the area of VWF self-association, PS binding was significantly higher than all other conditions. Error bars are standard deviation (SD). Statistical significance was determined with an analysis of variance (ANOVA) and Tukey post hoc test; n.s., nonsignificant; $^{**}P < .01$; $^{***}P < .001$; $^{****}P < .0001$. Scale bar, 25 µm. DIC, differential interference contrast, PDMS, polydimethylsiloxane.

Soluble VWF interacts with PS in plasma and blocks the measurement of free PS

Similar elevated VWF is common in the same conditions associated with free PS deficiency and loss of PS anticoagulant activity; we hypothesized that VWF binds PS in plasma and causes clinical PS deficiency. To test this hypothesis, VWF was sheared by vortexing, which induces VWF unfolding, and added to plasma at different concentrations (0, 10, 20, and 40 µg/mL) to mimic physiological (~10 µg/mL) and pathological concentrations (~40 µg/mL). For these experiments, VWF was vortexed for a shorter time (30 seconds) to prevent the loss of VWF and mimic milder unfolding conditions. In Figure 5A, VWF dose-dependently interfered with the detection of free but not total PS in pooled plasma. Similar vortexing of individual plasmas reduced free PS in all samples, although the extent of decrease varied between individuals (Figure 5B). The effect of vortexing was similar either in the absence or presence of calcium when measured with either purified proteins or plasma (Figure 5C). Vortexing for 30 seconds did not alter the VWF concentration in pooled normal plasmas or individual donor plasmas when measured with 2 different enzyme-linked immunosorbent assays, indicating that no significant loss of VWF occurs under these conditions (supplemental Figure 3).

To detect PS binding partners, we analyzed plasma on native, nondenaturing gels and probed for PS-containing complexes by immunoblotting (supplemental Figure 4A). Because free PS deficiency is prevalent in individuals with COVID-19,[18] patient plasma samples were compared with healthy control plasmas. As expected, purified PS appeared as 2 species on the native gels. PS dimerizes when at high concentrations (17 µM), and this dimerization is inhibited by calcium.[35,36] Addition of calcium to purified PS resulted in a loss of the lower band, whereas EDTA increased the lower band. Thus, the upper band is the apparent PS monomer (*), and the lower band is the apparent dimer (**). Plasma PS migrated in a pattern distinct from purified PS (left 3 lanes), with no species comigrating at the same apparent mobility as either the purified PS monomer or dimer. Instead, several new bands appeared, most above the monomer and many toward the top of the gel. The most intensely stained band comigrated with a band also detected by an anti–C4BP-β antibody (supplemental Figure 4B), consistent with reports that ~60% of PS is complexed with C4BP.[4] Other PS-positive bands comigrated with bands detected by antibodies that recognize other known PS-binding proteins (eg, Mer, protein C [PC], TFPI, and factor V; supplemental Figure 5) or VWF (supplemental Figure 4C), each of which migrated differently in plasma than with purified protein (supplemental Figure 6). Consistent with the native gel results, PS, derivatized with the biotin transfer reagent sulfo-*N*-hydroxy-succinimidyl-2-(6-[biotinamido]-2-(*p*-azidobenzamido)-hexanoamido) ethyl-1,3′-dithioproprionate (sulfo-SBED), interacted with multiple binding partners, including VWF, when supplemented into PS-immunodepleted plasma (supplemental Figure 7). Crosslinking was induced with exposure to UV light, biotinylated proteins were isolated with streptavidin-coated beads, and analyzed by immunoblotting. Conversely, sulfo-SBED-labeled VWF associated with PS when vortexed and supplemented into plasma from a patient with type 3 von Willebrand disease. Neither protein interacted nonspecifically with the streptavidin beads (supplemental Figure 8). Crosslinked complexes were too large to enter the gel under nonreducing conditions.

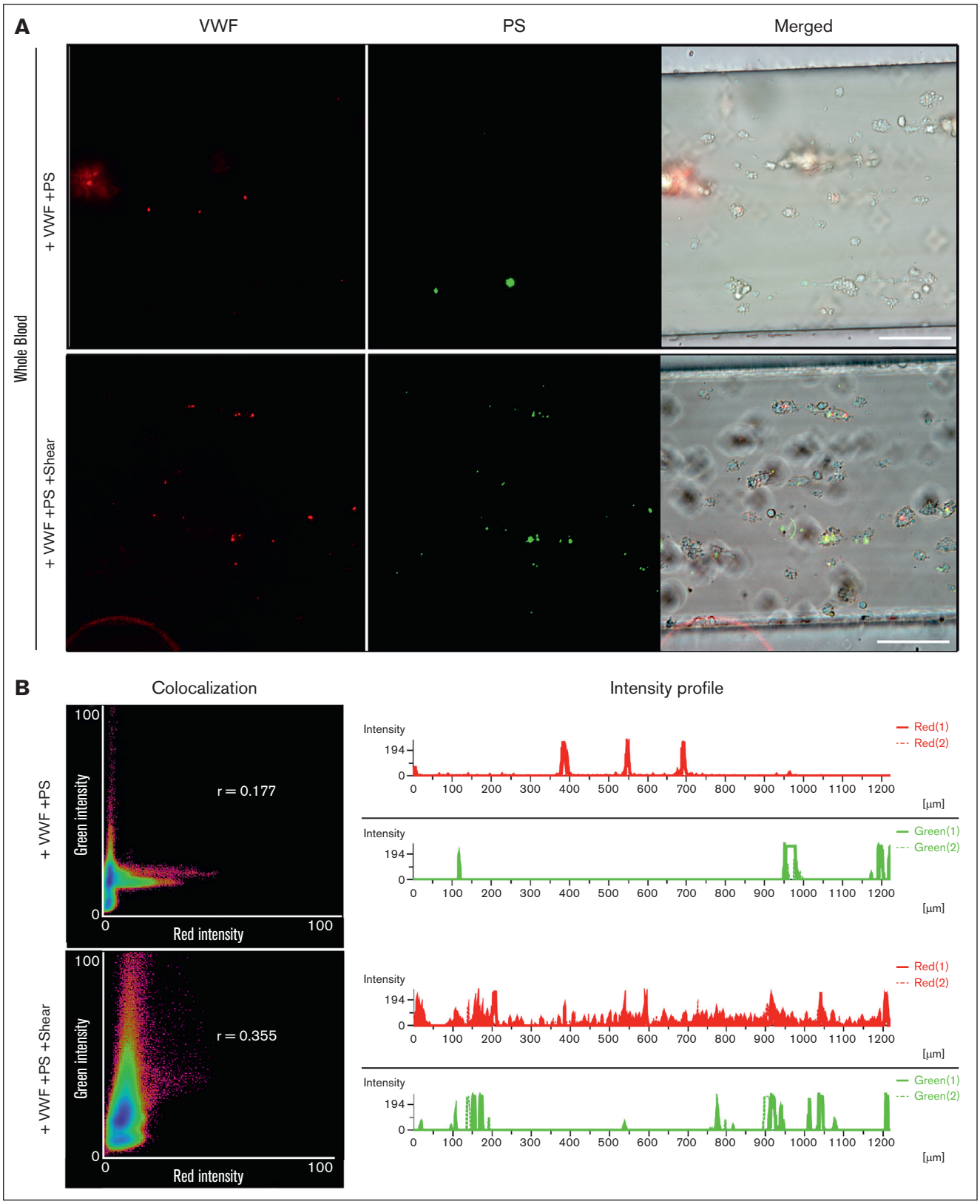

Figure 3. The PS/VWF complex is stable under flow. Whole blood was supplemented with 10 µg/mL AlexaFluor555-conjugated VWF and 200 nM AlexaFluor488-conjugated PS and perfused through collagen-coated channels at 35 dyn/cm^2. Experiments were performed either without or with PS/VWF vortexing. (A) Images taken after flushing with buffer; scale bar, 100 µm. (B) Colocalization (shown is Pearson correlation *r*) and intensity profile analyses using the Nikon Instruments Software Element software.

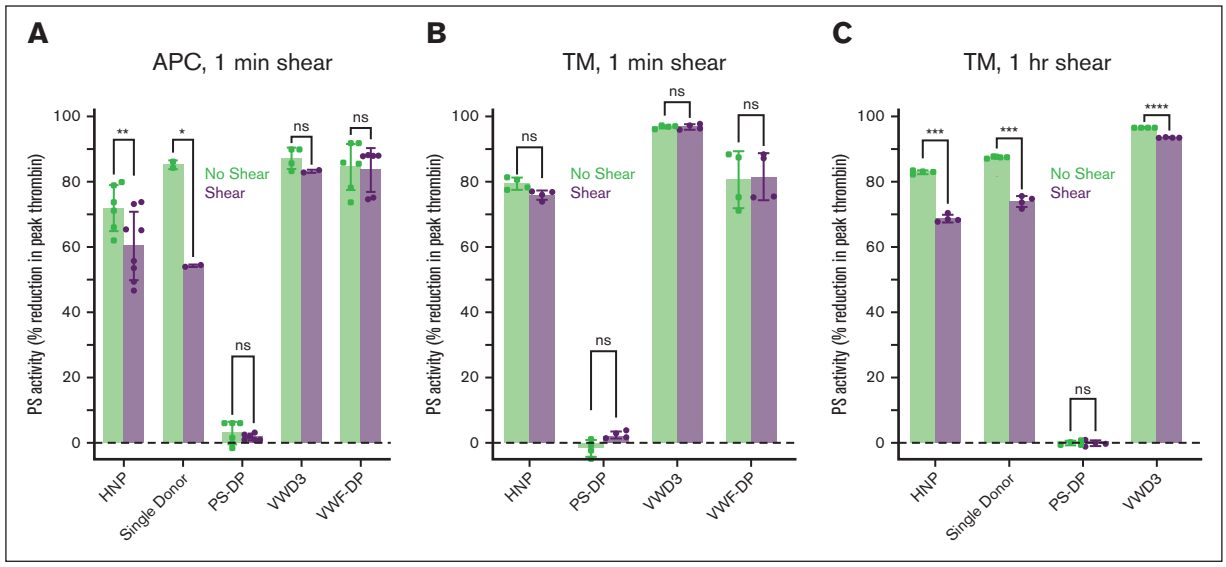

Figure 4. Unfolded VWF reduces PS plasma anticoagulant activity. Plasma thrombin generation was measured in pooled healthy normal plasma (HNP), single donor plasma, PS-DP, plasma from a patient with VWD3, or VWF-DP in the presence or absence of exogenous APC (5 nM; A) or thrombomodulin (20 nM; B-C) and the presence or absence of short-term shear (1 minute; A-B) or long-term shear (1 hour; C). Paired *t* tests were performed with each individual data set, comparing plasma with or without shearing; **P* < .05; ***P* < .01; ****P* < .001; *****P* < .001. PS-DP, PS-depleted plasma, VWD3, type 3 von Willebrand disease, VWF-DP, VWF-depleted plasma.

Finally, PS (~69 kDa as a monomer) was observed on VWF multimer gels (supplemental Figures 9 and 10) and ran as a ladder of bands, similar to that seen for VWF. Although the lowest molecular weight band migrated similarly to a complex with C4BP (supplemental Figure 10B), the remaining bands comigrated with the low molecular weight VWF multimers (supplemental Figure 9). This was apparent regardless of shearing or calcium supplementation, implying either the presence of preexisting PS/VWF complexes in plasma or that VWF unfolding in the electrophoretic buffer or system enabled PS binding. Overall, the results indicate that PS has multiple binding partners in plasma, apart from C4BP, including VWF.

VWF competes with TFPI but not APC for binding PS

To further define the PS/VWF interaction, we developed a PS/VWF complex enzyme-linked immunosorbent assay, in which VWF is captured by a polyclonal antibody and bound PS is detected with a second polyclonal antibody. Using this assay, captured VWF bound

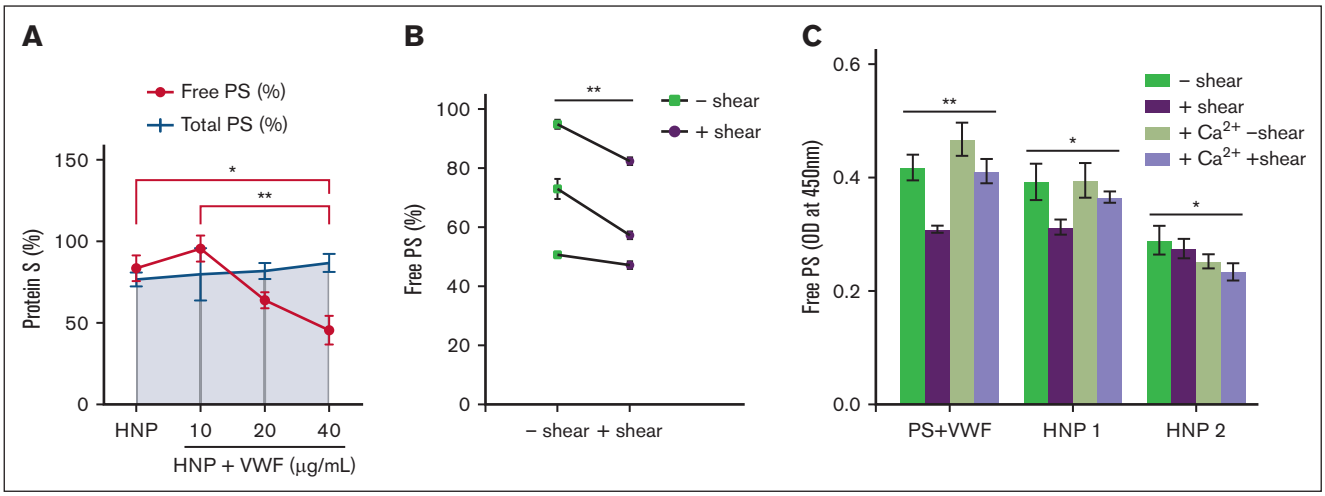

Figure 5. VWF reduces the measurement of free PS. (A) Free PS and total PS enzyme-linked immunosorbent assay (ELISA) measurements of HNP (from Siemens), with additions of purified VWF, under shear (~2500 rpm for 30 seconds). Free and total PS are presented as percent of free and total PS in reference plasma, respectively. (B) Free PS ELISA measurements of healthy control plasmas from single donors with or without shear. *P* values are according to Wilcoxon matched-pairs signed rank test; ***P* < .01. (C) Free PS ELISA results of purified proteins (200 nM PS and 10 μg/mL VWF in HEPES-buffered saline, with albumin), HNP1 (Corgenix), and HNP2 (Siemens), with or without shear or 1 μM hirudin, 5 mM Gly-Pro-Arg-Pro peptide, and 5 mM $CaCl_2$ supplementation; nondetectible. *P* values for panel A are according to 2-way ANOVA with Sidak multiple comparisons test. *P* values for panels B-C are according to Kruskal-Wallis with Dunn multiple comparison test; **P* < .05; ***P* < .01. OD, XXX; rpm, XXX.

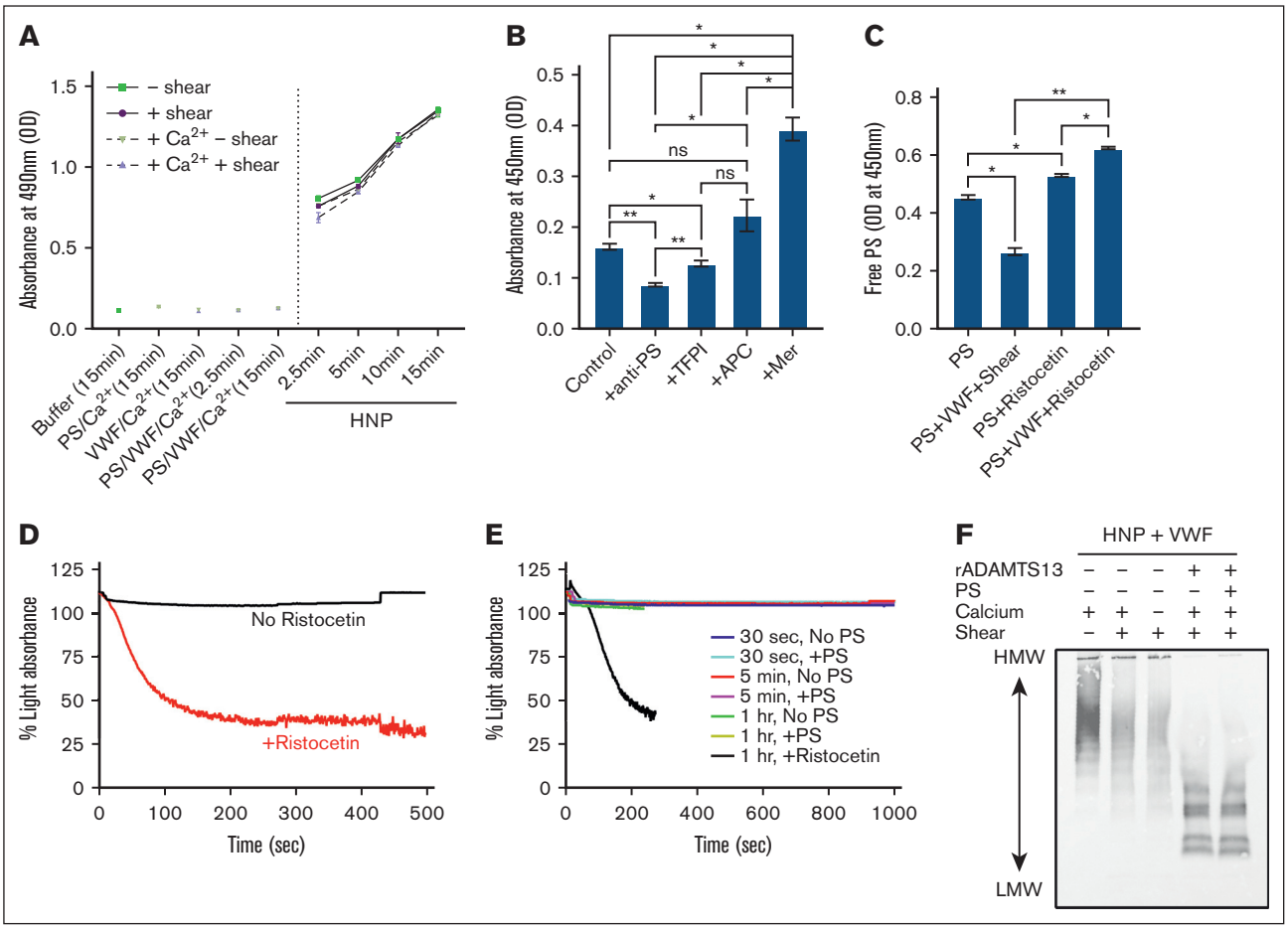

Figure 6. Direct measurement of the PS/VWF complex in plasma. (A) PS/VWF complex was measured by ELISA, using polyclonal antibodies to capture VWF and detect bound PS. Experiments were performed with purified proteins (200 nM PS, 10 μg/mL VWF, and 5 mM $CaCl_2$, as indicated, in HEPES-buffered saline, with albumin) or HNP, with or without shear or 1 μM hirudin, 5 mM Gly-Pro-Arg-Pro peptide, and 5 mM $CaCl_2$ supplementation. Samples were incubated on the plate for the indicated time. (B) Biotinylated PS (150 nM) was added to PS-immunodepleted plasma, and PS/VWF complex was detected as in panel A, except using streptavidin-HRP to detect. Experiments were performed in the presence or absence of saturating concentrations of an anti-PS polyclonal antibody, TFPIα, APC, or MerTK. (C) Free PS was measured, as in Figure 1, using purified PS (200 nM), with or without purified VWF (10 μg/mL) and ristocetin (2 mg/mL). (D-E) Washed platelets (2.5×10^8/mL) were aggregated in the presence or absence of VWF (10 μg/mL), PS (150 nM), and ristocetin (2 mg/mL). Experiments were performed in the absence (D) or presence (E) of vortexing to unfold VWF. In panel E, VWF was vortexed for 30 seconds, 5 minutes, or 1 hour. (F) VWF multimer blot of 0.25 μL HNP with additional 150 nM purified VWF, with or without 50 nM recombinant ADAMTS13, 200 nM PS, or 1 μM hirudin, 5 mM Gly-Pro-Arg-Pro peptide, and 5 mM $CaCl_2$, supplementation with or without shear (~2500 rpm for 60 minutes). Every data point is the average of 3 replicates (mean ± SD). *P* values for panels B-C are according to Kruskal-Wallis with Dunn multiple comparison test; $*P < .05$; $**P < .01$. For panels D-E, experiments were performed using platelets from 3 different donors. Shown are the average aggregation curves. HRP, horseradish peroxidase; rpm, revolutions per minute.

PS from plasma in a time-dependent manner (Figure 6A), consistent with VWF immobilization inducing exposure of protein binding sites.[37] Vortexing and calcium had no effect. Similarly, biotinylated PS bound to immobilized VWF, as detected with streptavidin-horseradish peroxidase (Figure 6B). Pretreatment with a polyclonal anti-PS antibody reduced the detection of the PS/VWF complex, as did the addition of saturating concentrations of TFPIα (Figure 6B). However, the addition of APC had no effect. These data suggest that VWF likely binds PS at or near the TFPIα binding site, which is located within the sex hormone–binding globulin (SHBG) region.[38] APC binds within the PS epidermal growth factor domains.[39-42] Saturating concentrations of mer tyrosine kinase (MerTK) increased PS detection (Figure 6B). Because MerTK preferentially binds dimerized PS,[43] the increase may reflect the presence of PS dimer or indicate that dimeric PS preferentially binds VWF.

The PS interaction site on VWF appears distinct from that which binds GPIb. Ristocetin had no effect on PS binding (Figure 6C) but did expose the platelet GPIb binding site on VWF, as measured by its ability to promote platelet aggregation (Figure 6D). By contrast, vortexing VWF, under the same conditions that allow PS binding, did not promote platelet aggregation (Figure 6E). This is consistent with a recent report that soluble VWF only induces platelet aggregation when exposed to shear forces higher than those used here.[44] Platelets did aggregate when ristocetin was added to VWF after 1-hour vortexing, indicating that vortexing VWF does not induce loss of VWF through aggregation or otherwise impair its function. Finally, exogenous PS did not interfere with VWF cleavage by ADAMTS13 (Figure 6F), which targets the unfolded A2 domain. Collectively, the data indicate that PS binds a shear-exposed site on VWF that is distinct from those that bind GPIb and ADAMTS13.

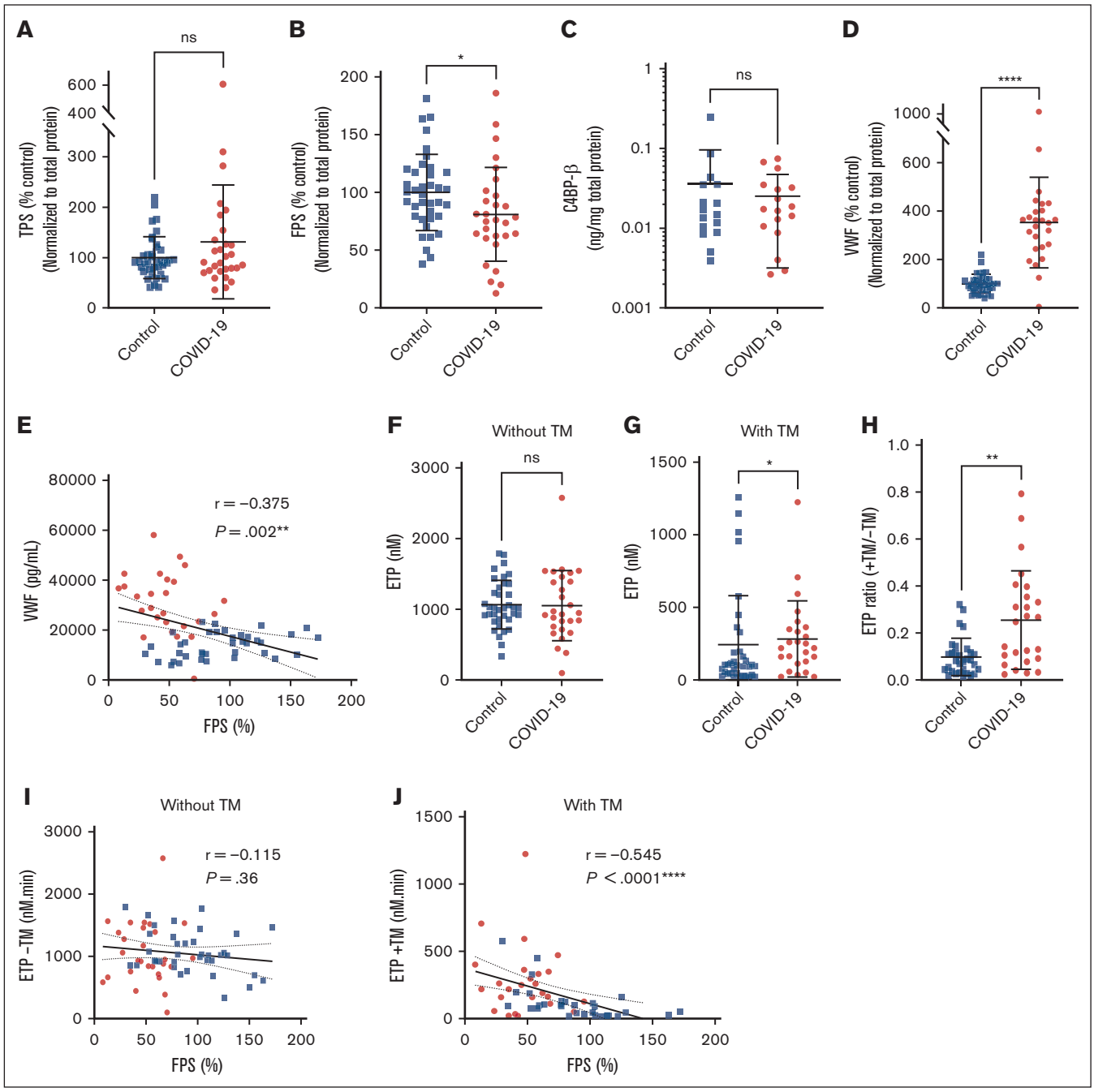

Figure 7. Free PS deficiency in patients with COVID-19 can be explained by changes in VWF but not C4BP. Citrated plasma samples were collected from healthy controls (n = 38) and patients with COVID-19 (n = 30). Due to sample limitations, some measurements could not be performed with all participants. (A-D) Total PS (A), free PS (B), C4BP-β (C), and VWF (D) were measured by ELISA. (E) Free PS plotted against VWF:Ag. (F-J) Plasma thrombin generation was measured using calibrated automated thrombography. Several patients were receiving heparin prophylactic dose at the time of blood collection. Shown are the ETPs in assays initiated with 4 μM phospholipids and 1 pM tissue factor (TF) (F) or with 20 nM thrombomodulin (TM) supplementation to evaluate the contribution of APC/PS activity (G), and the ETP ratio (value with TM/value without TM) (H). (I-J) Free PS plotted against ETP in the absence (I) or presence (J) of thrombomodulin. Every data point is the average of 3 replicates (mean ± SD). For panels A-H, *P* values are according to Mann-Whitney test; **P* < .05; ***P* < .01. For panels I-J, *P* values and *r* correlation coefficients are according to Spearman correlation analysis; ****P* < .001; *****P* < .0001. Blue squares represent controls, and red circles represent patients with COVID-19. FPS, XXX; TPS, XXX.

Free PS deficiency in patients with COVID-19 correlates with increased VWF and thrombin generation potential

To assess whether this interaction occurs in vivo, we analyzed plasma samples from a cohort of healthy controls (n = 38) and patients with severe COVID-19 (intensive care unit patients; n = 30), a condition associated with free PS deficiency.[18] As expected, samples from patients with COVID-19 exhibited elevated markers of infection, inflammation, and coagulopathy compared with controls (supplemental Figure 11), consistent with the hypercoagulable and hyperinflammatory state found in patients with COVID-19.[45-48]

Total PS was unchanged ($P = .611$; Figure 7A), but free PS (Figure 7B) decreased in patients (81% ± 40.6%) compared with controls (100% ± 33%; $P = .017$). The free PS deficiency could not be explained by C4BP, because C4BP-β (Figure 7C) was unchanged in patients nor by PC (supplemental Figure 12A) or soluble Mer-TK (supplemental Figure 12B). Plasma VWF antigen concentration (VWF:Ag) was elevated in the patients (353% ± 187%; $P < .0001$) compared with controls (100% ± 38.2%; Figure 7D), as others have previously reported.[49] Soluble E-selectin was also elevated (191 ± 72.5 pg/mg vs 133 ± 32 pg/mg total protein in patients vs controls; $P = .0001$), consistent with increased VWF secretion from activated endothelium (supplemental Figure 13A). VWF multimer distribution was unchanged (supplemental Figure 13B). VWF:Ag negatively correlated with free PS concentration ($r = -0.375$; $P = .002$; Figure 7E).

Finally, to assess the functional consequence of PS deficiency, plasma thrombin generation was measured in the presence or absence of thrombomodulin. Despite most patients receiving heparin prophylaxis at the time of sample collection, plasma thrombin generation was significantly elevated when measured in the presence of thrombomodulin (peak thrombin, $P = .01$; endogenous thrombin potential [ETP], $P = .043$) but not in its absence (Figure 7F-G; supplemental Figure 14). There was no difference between groups in the absence of exogenous tissue factor (supplemental Figure 14). The ETP ratio, defined as the value with thrombomodulin divided by that without thrombomodulin, was also increased in patients compared with controls (peak thrombin ratio; $P = .014$; ETP ratio; $P = .001$; Figure 7H). Consistent with our previous report,[11] free PS only weakly correlated with peak thrombin and did not correlate with ETP in the absence of thrombomodulin (Figure 7I; supplemental Figure 14E) but showed a strong negative correlation in the presence of thrombomodulin (peak thrombin, $r = -0.475$ [$P = .0002$]; ETP, $r = -0.545$ [$P < .0001$]; Figure 7J; supplemental Figure 14F), indicating a significant functional consequence of the free PS deficiency–reduced APC/PS pathway activity. Thus, free PS deficiency in this population is consistent with a mechanism in which increased, unfolded VWF binds PS, blocks anticoagulant activity, and blocks free PS measurement.

Discussion

Free PS deficiency is a common complication of severe viral infections, including HIV-1, dengue, varicella, and COVID-19.[10-17,19] The specific decrease in free PS indicates a concurrent increase in a PS-binding protein, with C4BP being the best-known candidate. The major isoform (~80%) of C4BP contains 7α chains and 1β chain, with the other isoforms containing either 6α and 1β or exclusively 7α or 6α.[50] The β chain binds PS.[51,52] Although C4BP is commonly increased during infection and inflammation, this change is mostly associated with elevated α chain, suggesting that the acute phase C4BP is unlikely to bind PS.[21] Thus, we hypothesized that another plasma protein is altered during inflammation, binds PS, reduces "free PS" concentration, and reduces PS anticoagulant activity. Our attention focused on VWF, because VWF is elevated in disease states that often present with PS deficiency.[22-25] VWF also precipitates in PEG,[53] which has been historically used to separate the free and bound pools of PS.[20] Here, we showed that VWF binds PS in a shear-dependent manner, blocks free PS measurement, and reduces PS anticoagulant activity. Furthermore, PS binds VWF as it unfolds dynamically under flow and forms a stable complex that associates with platelet thrombi. Finally, PS deficiency in a cohort of patients with COVID-19 is consistent with alterations in VWF but not C4BP. Based on these data, we propose that dysfunctional VWF directly sequesters PS, promoting thrombin generation through the reduction of available anticoagulant activity. This is a heretofore unrecognized procoagulant activity of VWF and, to our knowledge, the first description of anticoagulant regulation by VWF.

Our study began with the identification of PS as a shear-dependent, plasma VWF binding partner by mass spectrometry (Figure 1). Consistent with the mass spectrometry results, purified PS bound to VWF that unfolded and self-associated under turbulent shear flow conditions (Figure 2), as hypothesized to occur in patients with severe inflammation.[54] In contrast, this complex did not form under arterial laminar flow (Figure 3). However, when preformed, the PS/VWF complex was stable in recalcified whole blood and colocalized on platelet thrombi under arterial laminar flow. Thus, elevated and/or turbulent shear forces appear to be required to expose a PS-binding site on VWF, and PS did not interfere with the VWF/platelet interaction. These data also suggest that VWF may alter PS anticoagulant activity on the activated platelet surface.

VWF reduced PS anticoagulant activity in 2 different plasma thrombin generation assays (Figure 4). Vortexing plasma resulted in a consistent ~10% decrease in the anticoagulant effect of exogenous APC, an effect dependent on PS and VWF. Similarly, extended vortexing of plasma reduced the anticoagulant effect of exogenous thrombomodulin, an activity that was again dependent on PS and VWF. The thrombomodulin results indicate a time-dependence to the effect, in which VWF must be unfolded and able to bind PS at the time that APC is available. Under short-term shear conditions, VWF likely refolds during the 10-minute incubation time of the thrombin generation assay. Upon exposure to prolonged shear, similar to that likely occurring in patients with chronic inflammation, sufficient VWF remains unfolded and/or bound to PS to reduce anticoagulant activity. To our knowledge, this is the first evidence of a direct effect of VWF regulating plasma anticoagulant function. Mouse models may provide a valuable tool to study the effects of VWF activity in vivo, because mice lack C4BP-β,[55] and *vwf*$^{-/-}$ mice are viable,[56] providing a means to study PS activity in the presence or absence of these 2 PS-binding proteins.

To further understand the PS/VWF interaction, we visualized PS in plasma from patients with COVID-19, a population with well-described acquired free PS deficiency,[18] and healthy controls by nondenaturing gel electrophoresis and immunoblotting

(supplemental Figure 4). A multitude of bands toward the top of the gel were observed in all plasma samples, suggesting that PS circulates in plasma bound to many other proteins. Most of these interactions are likely of lower affinity than C4BP and, thus, were not identified in previous studies using size exclusion chromatography.[4] Some of the PS bands on the native gel comigrated with VWF. Purified PS and VWF were also labeled with the sulfo-SBED biotin transfer reagent and found to crosslink to plasma VWF and PS, respectively, when exposed to shear. Sheared VWF dose-dependently decreased the measurement of free PS, as did shearing plasma (Figure 5).

Our data suggest that the VWF binding site on PS is likely adjacent to or sterically hindered by the C4BP-binding site, which is found within the C-terminal SHBG region, because this is the epitope recognized by the monoclonal antibody used to measure free PS,[57] and C4BP-β chain was not detected by either mass spectrometry or immunoblotting (Figure 1). Consistent with this, saturating concentrations of TFPIα, which also binds the SHBG region,[38] competed with VWF for binding PS (Figure 6B). APC, which binds the N-terminal epidermal growth factor domains,[39-42] had no effect. Interestingly, the apparent interaction of PS with VWF was increased approximately twofold in the presence of MerTK. Because MerTK binds dimeric PS,[43] this increase may reflect dimerization of PS and not an actual increase in binding affinity for VWF. However, the data do indicate that the VWF and MerTK binding sites are distinct. PS promotes the complement inhibitory function of C4BP and is a bridging molecule for efferocytosis through its interaction with MerTK and other phagocytic cell receptors. The effect of VWF on these pathways is unknown. Our data indicate that the PS/VWF complex interacts with MerTK and thus may still interact with macrophages and other phagocytic cells. However, since PS binding induces anti-inflammatory signaling in macrophages, while VWF binding induces pro-inflammatory signals, the net result of the PS/VWF complex is currently unclear.

The exact PS binding site on VWF is unknown; however, it is distinct from the GPIb binding site, because treatment with ristocetin, which exposes that site, did not reduce free PS (Figure 6C-D). Consistent with this, the shear stress we exerted by vortexing, which exposed the PS binding site, did not stably expose the platelet binding site (Figure 6E). Finally, calcium disrupts the PS/VWF interaction (Figure 2), an observation with 2 evident interpretations: first, calcium stabilizes the folded state of A2,[31,33] and thus, PS may bind unfolded A2; second, calcium disrupts PS dimerization. Either or both mechanisms are consistent with our data. An interaction with A2 would also be consistent with the presence of PS on VWF multimer gels (supplemental Figure 9), because PS may interact with terminal A2 fragments, exposed in smaller VWF multimers generated through cleavage by ADAMTS13. Consistent with this hypothesis, PS was most readily detected on low molecular weight VWF multimers, which have a relatively higher abundance of terminal A2 fragments, and its intensity decreased as multimer size increased (supplemental Figures 9 and 10). The effect of calcium also suggests that the PS/VWF interaction may more readily form under conditions of hypocalcemia, as have been reported in patients with COVID-19.[58,59]

Our data offer an explanation for free PS deficiency during infections. Free PS deficiency was prevalent in our COVID-19 population and correlated with elevated plasma thrombin generation, which was elevated in patients in the presence of thrombomodulin (Figure 7). Free PS deficiency could not be explained by alterations in C4BP-β but were consistent with the proposed VWF-mediated mechanism, because VWF was elevated in patients and inversely correlated with free PS. Because shearing reduces free PS in healthy control plasma, the effect of VWF on free PS is likely mediated by shear-dependent unfolding of VWF, rather than by changes in VWF antigen. Unfolding and self-association of VWF are favored in regions of flow acceleration, such as that occurring in stenotic arteries or valves and in resistance vessels,[60] especially during hypertension. It is noteworthy that in 2 studies published early in the COVID-19 pandemic, hypertension was the most common comorbidity associated with severe disease.[46,61] Hypertension is also associated with reduced PS.[62]

In conclusion, we propose a model in which shear-induced unfolding exposes a binding site on VWF, possibly within the A2 domain, that directly interacts with PS, likely within the SHBG domain. VWF binding reduces PS anticoagulant activity and blocks the measurement of free PS. This proposed mechanism is consistent with the free PS deficiency that develops in COVID-19 and with historic measurements of free PS deficiency, which is prevalent in inflammatory conditions that are also associated with VWF dysfunction and which relied on PEG precipitation of plasma, a process also used to precipitate VWF. We anticipate that this mechanism broadly contributes to acquired free PS deficiency in inflammatory conditions in which VWF is exposed to elevated vascular shear force and thereby contributes to the prothrombotic state. Finally, VWF binding may modulate PS anticoagulant activity under normal hemostatic conditions when VWF unfolds at the site of vascular injury. Unfolded VWF may serve to sequester PS and limit its anticoagulant activity within the context of a platelet plug.

Acknowledgments

The authors thank Etheresia Pretorius for her advice about the thioflavin T procedure.

This study was supported by National Heart, Lung, and Blood Institute grants HL150818 (S.W.W.), HL129193 (J.P.W.), HL145262 (J.A.L.), HL007093 (M.Y.M.), Department of Veterans Affairs Merit I01BX003877 (S.W.W.), and University of Kentucky Center for Clinical and Translational Science pilot grants (J.G.W. and J.P.W.). The University of Kentucky Flow Cytometry & Immune Monitoring core facility is supported in part by the Office of the Vice President for Research, the Markey Cancer Center, and an National Cancer Institute Center Core support grant (P30 CA177558). This study was supported by the National Center for Research Resources and the National Center for Advancing Translational Sciences, National Institutes of Health, through grant UL1TR001998.

Authorship

Contribution: M.M.S.S. and J.P.W. designed and performed experiments, analyzed data, and wrote the first draft of the manuscript; M.Y.M., H.R.A., M.H., D.W.C., X.F., S.G., D.M.C., K.S.P., M.B., C.P., and X.L. designed and performed experiments and analyzed data; J.P.W., J.A.L., J.G.W., B.A.G., and S.W.W. designed the study and critically revised the manuscript; D.W.C., D.F.D., and Z.Z. critically revised the manuscript; A.C.T., J.Z.P., J.L.S., G.A.S., M.B.-B., and K.S.C. recruited the patients; and all authors reviewed the final version of the manuscript and approved its submission.

Conflict-of-interest disclosure: J.P.W. received an investigator-initiated grant through Pfizer Inc, unrelated to this project. The remaining authors declare no competing financial interests.

ORCID profiles: M.M.S.S., 0000-0002-6966-1494; M.Y.M., 0000-0002-5975-3539; H.R.A., 0000-0003-4668-4367; S.G., 0000-0002-0764-1308; D.M.C., 0000-0001-9036-9685; M.B., 0000-0002-5139-5861; C.P., 0000-0002-6761-5566; J.L.S., 0000-0001-8856-3227; Z.Z., 0000-0002-4453-224X; S.W.W., 0000-0001-5577-0473; B.A.G., 0000-0002-7756-6921; J.P.W., 0000-0001-5487-852X.

Correspondence: Jeremy P. Wood, The Gill Heart and Vascular Institute, University of Kentucky, 741 S Limestone, BBSRB B359, Lexington, KY 40508; email: jeremy.wood@uky.edu.

References

1. Mann KG, Nesheim ME, Church WR, Haley P, Krishnaswamy S. Surface-dependent reactions of the vitamin K-dependent enzyme complexes. *Blood*. 1990;76(1):1-16.
2. Calzavarini S, Prince-Eladnani R, Saller F, et al. Platelet protein S limits venous but not arterial thrombosis propensity by controlling coagulation in the thrombus. *Blood*. 2020;135(22):1969-1982.
3. Mahasandana C, Suvatte V, Marlar RA, Manco-Johnson MJ, Jacobson LJ, Hathaway WE. Neonatal purpura fulminans associated with homozygous protein S deficiency. *Lancet*. 1990;335(8680):61-62.
4. Dahlbäck B, Stenflo J. High molecular weight complex in human plasma between vitamin K-dependent protein S and complement component C4b-binding protein. *Proc Natl Acad Sci U S A*. 1981;78(4):2512-2516.
5. Walker FJ. Regulation of activated protein C by protein S. The role of phospholipid in factor Va inactivation. *J Biol Chem*. 1981;256(21):11128-11131.
6. Wood JP, Ellery PER, Maroney SA, Mast AE. Protein S is a cofactor for platelet and endothelial tissue factor pathway inhibitor-α but not for cell surface–associated tissue factor pathway inhibitor. *Arterioscler Thromb Vasc Biol*. 2014;34(1):169-176.
7. Chattopadhyay R, Sengupta T, Majumder R. Inhibition of intrinsic Xase by protein S: a novel regulatory role of protein S independent of activated protein C. *Arterioscler Thromb Vasc Biol*. 2012;32(10):2387-2393.
8. Denis CV, Roberts SJ, Hackeng TM, Lenting PJ. In vivo clearance of human protein S in a mouse model: influence of C4b-binding protein and the Heerlen polymorphism. *Arterioscler Thromb Vasc Biol*. 2005;25(10):2209-2215.
9. Dahlback B. Inhibition of protein Ca cofactor function of human and bovine protein S by C4b-binding protein. *J Biol Chem*. 1986;261(26):12022-12027.
10. Bissuel F, Berruyer M, Causse X, Dechavanne M, Trepo C. Acquired protein S deficiency: correlation with advanced disease in HIV-1-infected patients. *J Acquir Immune Defic Syndr (1988)*. 1992;5(5):484-489.
11. Sim MMS, Banerjee M, Myint T, Garvy BA, Whiteheart SW, Wood JP. Total plasma protein S is a prothrombotic marker in people living with HIV. *J Acquir Immune Defic Syndr*. 2022;90(4):463-471.
12. Nguyên P, Reynaud J, Pouzol P, Munzer M, Richard O, François P. Varicella and thrombotic complications associated with transient protein C and protein S deficiencies in children. *Eur J Pediatr*. 1994;153(9):646-649.
13. Wills BA, Oragui EE, Stephens AC, et al. Coagulation abnormalities in dengue hemorrhagic fever: serial investigations in 167 Vietnamese children with dengue shock syndrome. *Clin Infect Dis*. 2002;35(3):277-285.
14. Ali L, Jamoussi H, Kouki N, et al. COVID-19 infection and recurrent stroke in young patients with protein S deficiency: a case report. *Neurologist*. 2021;26(6):276-280.
15. Baicus C, Stoichitoiu LE, Pinte L, Badea C. Anticoagulant protein S in COVID-19: the low activity level is probably secondary. *Am J Ther*. 2021;28(1):e139-e140.
16. Ferrari E, Sartre B, Squara F, et al. High prevalence of acquired thrombophilia without prognosis value in patients with coronavirus disease 2019. *J Am Heart Assoc*. 2020;9(21):e017773.
17. Lemke G, Silverman GJ. Blood clots and TAM receptor signalling in COVID-19 pathogenesis. *Nat Rev Immunol*. 2020;20(7):395-396.
18. Sim MMS, Wood JP. Dysregulation of protein S in COVID-19. *Best Pract Res Clin Haematol*. 2022;35(3):101376.
19. Stoichitoiu LE, Pinte L, Balea MI, Nedelcu V, Badea C, Baicus C. Anticoagulant protein S in COVID-19: low activity, and associated with outcome. *Rom J Intern Med*. 2020;58(4):251-258.
20. Woodhams BJ. The simultaneous measurement of total and free protein S by ELISA. *Thromb Res*. 1988;50(1):213-220.
21. Garcia de Frutos P, Alim RI, Hardig Y, Zoller B, Dahlback B. Differential regulation of alpha and beta chains of C4b-binding protein during acute-phase response resulting in stable plasma levels of free anticoagulant protein S. *Blood*. 1994;84(3):815-822.
22. Graham SM, Chen J, Le J, et al. Von Willebrand factor adhesive activity and ADAMTS13 protease activity in HIV-1-infected men. *Int J Med Sci*. 2019;16(2):276-284.
23. Grobler C, Maphumulo SC, Grobbelaar LM, et al. Covid-19: the rollercoaster of fibrin(Ogen), D-Dimer, von Willebrand factor, P-selectin and their interactions with endothelial cells, platelets and erythrocytes. *Int J Mol Sci*. 2020;21(14):5168.
24. Page AV, Liles WC. Biomarkers of endothelial activation/dysfunction in infectious diseases. *Virulence*. 2013;4(6):507-516.

25. van den Dries LW, Gruters RA, Hovels-van der Borden SB, et al. von Willebrand factor is elevated in HIV patients with a history of thrombosis. *Front Microbiol*. 2015;6:180.

26. Li F, Li CQ, Moake JL, López JA, McIntire LV. Shear stress-induced binding of large and unusually large von Willebrand factor to human platelet glycoprotein Ibalpha. *Ann Biomed Eng*. 2004;32(7):961-969.

27. Zanardelli S, Chion AC, Groot E, et al. A novel binding site for ADAMTS13 constitutively exposed on the surface of globular VWF. *Blood*. 2009; 114(13):2819-2828.

28. Zlobina KE, Guria GT. Platelet activation risk index as a prognostic thrombosis indicator. *Sci Rep*. 2016;6:30508.

29. Banerjee M, Huang Y, Joshi S, et al. Platelets endocytose viral particles and are activated via TLR (toll-like receptor) signaling. *Arterioscler Thromb Vasc Biol*. 2020;40(7):1635-1650.

30. Chung DW, Chen J, Ling M, et al. High-density lipoprotein modulates thrombosis by preventing von Willebrand factor self-association and subsequent platelet adhesion. *Blood*. 2016;127(5):637-645.

31. Jakobi AJ, Mashaghi A, Tans SJ, Huizinga EG. Calcium modulates force sensing by the von Willebrand factor A2 domain. *Nat Commun*. 2011;2:385.

32. Sugo T, Dahlback B, Holmgren A, Stenflo J. Calcium binding of bovine protein S. Effect of thrombin cleavage and removal of the gamma-carboxyglutamic acid-containing region. *J Biol Chem*. 1986;261(11):5116-5120.

33. Xu AJ, Springer TA. Calcium stabilizes the von Willebrand factor A2 domain by promoting refolding. *Proc Natl Acad Sci U S A*. 2012;109(10): 3742-3747.

34. Brugge JM, Tans G, Rosing J, Castoldi E. Protein S levels modulate the activated protein C resistance phenotype induced by elevated prothrombin levels. *Thromb Haemost*. 2006;95(2):236-242.

35. Pauls JE, Hockin MF, Long GL, Mann KG. Self-association of human protein S. *Biochemistry*. 2000;39(18):5468-5473.

36. Seré KM, Janssen MP, Willems GM, Tans G, Rosing J, Hackeng TM. Purified protein S contains multimeric forms with increased APC-independent anticoagulant activity. *Biochemistry*. 2001;40(30):8852-8860.

37. Li CQ, Dong JF, López JA. The mucin-like macroglycopeptide region of glycoprotein Ibalpha is required for cell adhesion to immobilized von Willebrand factor (VWF) under flow but not for static VWF binding. *Thromb Haemost*. 2002;88(4):673-677.

38. Reglinska-Matveyev N, Andersson HM, Rezende SM, et al. TFPI cofactor function of protein S: essential role of the protein S SHBG-like domain. *Blood*. 2014;123(25):3979-3987.

39. Andersson HM, Arantes MJ, Crawley JT, et al. Activated protein C cofactor function of protein S: a critical role for Asp95 in the EGF1-like domain. *Blood*. 2010;115(23):4878-4885.

40. Dahlback B, Hildebrand B, Malm J. Characterization of functionally important domains in human vitamin K-dependent protein S using monoclonal antibodies. *J Biol Chem*. 1990;265(14):8127-8135.

41. Mille-Baker B, Rezende SM, Simmonds RE, Mason PJ, Lane DA, Laffan MA. Deletion or replacement of the second EGF-like domain of protein S results in loss of APC cofactor activity. *Blood*. 2003;101(4):1416-1418.

42. Stenberg Y, Drakenberg T, Dahlback B, Stenflo J. Characterization of recombinant epidermal growth factor (EGF)-like modules from vitamin-K-dependent protein S expressed in Spodoptera cells–the cofactor activity depends on the N-terminal EGF module in human protein S. *Eur J Biochem*. 1998;251(3):558-564.

43. Uehara H, Shacter E. Auto-oxidation and oligomerization of protein S on the apoptotic cell surface is required for Mer tyrosine kinase-mediated phagocytosis of apoptotic cells. *J Immunol*. 2008;180(4):2522-2530.

44. Schneider MF, Fallah MA, Mess C, et al. Platelet adhesion and aggregate formation controlled by immobilised and soluble VWF. *BMC Mol Cell Biol*. 2020;21(1):64.

45. Tang N, Li D, Wang X, Sun Z. Abnormal coagulation parameters are associated with poor prognosis in patients with novel coronavirus pneumonia. *J Thromb Haemost*. 2020;18(4):844-847.

46. Zhou F, Yu T, Du R, et al. Clinical course and risk factors for mortality of adult inpatients with COVID-19 in Wuhan, China: a retrospective cohort study. *Lancet*. 2020;395(10229):1054-1062.

47. Zhang L, Yan X, Fan Q, et al. D-dimer levels on admission to predict in-hospital mortality in patients with Covid-19. *J Thromb Haemost*. 2020;18(6): 1324-1329.

48. Klok FA, Kruip MJHA, van der Meer NJM, et al. Incidence of thrombotic complications in critically ill ICU patients with COVID-19. *Thromb Res*. 2020; 191:145-147.

49. Pretorius E, Venter C, Laubscher GJ, et al. Prevalence of symptoms, comorbidities, fibrin amyloid microclots and platelet pathology in individuals with long COVID/post-acute sequelae of COVID-19 (PASC). *Cardiovasc Diabetol*. 2022;21(1):148.

50. Blom AM, Villoutreix BO, Dahlbäck B. Complement inhibitor C4b-binding protein-friend or foe in the innate immune system? *Mol Immunol*. 2004; 40(18):1333-1346.

51. Carlsson S, Dahlback B. Dependence on vitamin K-dependent protein S for eukaryotic cell secretion of the beta-chain of C4b-binding protein. *J Biol Chem*. 2010;285(42):32038-32046.

52. Dahlback B. Protein S and C4b-binding protein: components involved in the regulation of the protein C anticoagulant system. *Thromb Haemost*. 1991; 66(1):49-61.

53. Kao KJ, Pizzo SV, McKee PA. Demonstration and characterization of specific binding sites for factor VIII/von Willebrand factor on human platelets. *J Clin Invest*. 1979;63(4):656-664.

54. Sarkar M, Madabhavi IV, Quy PN, Govindagoudar MB. COVID-19 and coagulopathy. *Clin Respir J*. 2021;15(12):1259-1274.

55. Rodriguez de Cordoba S, Perez-Blas M, Ramos-Ruiz R, Sanchez-Corral P, Pardo-Manuel de Villena F, Rey-Campos J. The gene coding for the beta-chain of C4b-binding protein (C4BPB) has become a pseudogene in the mouse. *Genomics*. 1994;21(3):501-509.

56. Denis C, Methia N, Frenette PS, et al. A mouse model of severe von Willebrand disease: defects in hemostasis and thrombosis. *Proc Natl Acad Sci U S A*. 1998;95(16):9524-9529.

57. Evenäs P, García De Frutos P, Linse S, Dahlbäck B. Both G-type domains of protein S are required for the high-affinity interaction with C4b-binding protein. *Eur J Biochem*. 1999;266(3):935-942.

58. Deodatus JA, Kooistra SA, Kurstjens S, et al. Lower plasma calcium associated with COVID-19, but not with disease severity: a two-centre retrospective cohort study. *Infect Dis (Lond)*. 2022;54(2):90-98.

59. Ruiz-Alvarez MJ, Stampone E, Verduras YF, et al. Hypocalcemia: a key biomarker in hospitalized COVID-19 patients. *Biomed J*. 2023;46(1):93-99.

60. Zheng Y, Chen J, López JA. Flow-driven assembly of VWF fibres and webs in in vitro microvessels. *Nat Commun*. 2015;6:7858.

61. Wu C, Chen X, Cai Y, et al. Risk factors associated with acute respiratory distress syndrome and death in patients with coronavirus disease 2019 pneumonia in Wuhan, China. *JAMA Intern Med*. 2020;180(7):934-943.

62. Vogel von Falckenstein J, Freuer D, Peters A, Heier M, Linseisen J, Meisinger C. Sex-specific associations between systolic, diastolic and pulse pressure and hemostatic parameters in the population-based KORA-Fit study: a cross-sectional study. *Thromb J*. 2023;21(1):7.